A METHODOLOGY FOR THE AUTOMATED OPTIMAL CONTROL OF FLOWS INCLUDING TRANSITIONAL FLOWS

Ronald D. Joslin
NASA Langley Research Center
Hampton, VA 23681

Max D. Gunzburger
Iowa State University
Ames, IA 50011

Roy A. Nicolaides
Carnegie Mellon University
Pittsburgh, PA 15213

Gordon Erlebacher
ICASE
Hampton, VA 23681

M. Yousuff Hussaini
Florida State University
Tallahassee, FL 32306

ABSTRACT

This paper describes a self-contained, automated methodology for active flow control which couples the time-dependent Navier-Stokes system with the adjoint Navier-Stokes system and optimality conditions from which optimal states, i.e., unsteady flow fields and controls (e.g., actuators), may be determined. The problem of boundary layer instability suppression through wave cancellation is used as the initial validation case to test the methodology. Here, the objective of control is to match the wall-normal stress along a portion of the boundary to a given vector; instability suppression is achieved by choosing the given vector to be that of a steady base flow. Control is effected through the injection or suction of fluid through a single orifice on the boundary. The results demonstrate that instability suppression can be achieved without any a priori knowledge of the disturbance. The present methodology may potentially be applied to separation control, re-laminarization, and turbulence control applications using one or more sensors and actuators.

1. INTRODUCTION

In the last decade, increasing attention has been devoted to the development of techniques capable of enhancing our ability to control the unsteady flow in a wide variety of configurations such as engine inlets and nozzles, combustors, automobiles, aircraft, and marine vehicles. Controlling the flow in these configurations can lead to greatly improved efficiency and performance, while decreasing the noise levels generally associated with the otherwise unattended unsteady flow. Depending on the desired result, one might wish to delay *or* accelerate transition, reduce drag *or* enhance mixing. There might be a need to postpone flow separation, increase lift or manipulate a turbulence field. Gad-el-Hak (1989) and Gad-el-Hak & Bushnell (1991) provide an excellent introduction to and overview of various control methodologies.

The methodology of the current paper is based on defining a control mechanism and an objective for control, and then finding, in a systematic and automated manner, controls that best meet the objective. In the present setting, an objective or cost functional is defined that measures the "distance" between the measured stresses, and their desired values along a limited section of the bounding wall and over a specified length of time. One may interpret the objective functional as a "sensor," i.e. the objective functional senses how far the flow stresses on the wall are from the corresponding desired values. To control the flow, time-dependent injection and suction is imposed along a small orifice in the bounding wall. Although the spatial dependence of the suction profile is specified (for simplicity), the optimal control methodology determines the time-variation of this profile. However, unlike feedback control methodologies wherein the sensed data determines the control through a specified feedback law or controller, here the time-dependence of the control is the natural result of the minimization of the objective functional. We have a sensor that feeds information to a controller that in turn feeds information to the actuator. However, in the optimal control setting, the sensor is actually an objective functional and the controller is a coupled system of partial differential equations that determine the control that does the best job of minimizing the objective functional.

The present active-control approach is demonstrated for the evolution and automated control of spatially grow-

ing 2D disturbances in a flat-plate boundary layer. As the length of time over which the minimization process is increased, we recover the results obtained by wave cancellation, thus validating the approach. The ultimate goal of this line of research is to introduce automated control to external flows over realistic configurations such as wings and fuselages, and to devise novel flow control techniques.

2. THE OPTIMIZATION PROBLEM

Due to restrictions on the length of this paper, an abbreviated derivation of the governing equations is listed below. For a detailed description of the derivation refer to Joslin et al. (1995), where both the channel and boundary-layer problems are outlined and both the wall-normal and shear stresses are included in the solution procedure. Here, only the wall-normal stress terms are included in the optimization problem for the boundary layer.

2.1. The state equations

Let Ω denote the flow domain which is the boundary layer $[x \geq 0,\ 0 \leq y \leq h]$, where h is the location of the truncated freestream condition. Let Γ denote its boundary and let $(0,T)$ be the time interval of interest. The inflow part of the boundary $[x = 0, 0 \leq y \leq h]$ is denoted by Γ_i and the upper boundary $[x \geq 0,\ y = h]$ is denoted by Γ_e. The part of the boundary on which control is applied (i.e., along which the actuator is placed) is denoted by Γ_a, which is assumed to be a finite connected part of Γ_w, which is the remaindor of the lower boundary (or wall) $[x \geq 0,\ y = 0]$. Controls are only activated over the given time interval $t \in (T_0, T_1)$, where $0 \leq T_0 < T_1 \leq T$.

The flow field is described by the velocity vector (u, v) and the scalar pressure p and is obtained by solving the following momentum and mass conservation equations:

$$\frac{\partial u}{\partial t} + u\frac{\partial u}{\partial x} + v\frac{\partial u}{\partial y} + \frac{\partial p}{\partial x} - \nu\frac{\partial^2 u}{\partial x^2} - \nu\frac{\partial^2 u}{\partial y^2} = 0 \qquad (1)$$

$$\frac{\partial v}{\partial t} + u\frac{\partial v}{\partial x} + v\frac{\partial v}{\partial y} + \frac{\partial p}{\partial y} - \nu\frac{\partial^2 v}{\partial x^2} - \nu\frac{\partial v^2}{\partial y^2} = 0 \qquad (2)$$

$$\frac{\partial u}{\partial x} + \frac{\partial v}{\partial y} = 0 \qquad (3)$$

in $(0,T)\times\Omega$ and subject to initial and boundary conditions:

$$u, v\big|_{t=0} = u_0, v_0 \quad \text{in } \Omega \qquad (4)$$

$$u, v\big|_{\Gamma_a} = \begin{cases} 0, g_2 & \text{in } (T_0, T_1) \\ 0, 0 & \text{in } (0, T_0) \text{ and } (T_1, T) \end{cases} \qquad (5)$$

$$u, v\big|_{\Gamma_i} = u_i, v_i; \quad u, v\big|_{\Gamma_w} = 0, 0 \quad \text{in } (0,T) \qquad (6)$$

$$u|_{\Gamma_e} = U_\infty \text{ and } (p - 2\nu\frac{\partial v}{\partial y})\Big|_{\Gamma_e} = P_\infty \text{ in } (0,T) \qquad (7)$$

where U_∞ and P_∞ denote the free-stream flow speed and pressure, respectively. Here, the initial velocity vector and the inflow velocity vector are assumed given and the base flow is assumed to be the Blasius similarity solution.

The control function $g_2(t,x)$ which gives the rate at which fluid is injected or sucked perpendicularly through Γ_a is to be determined as part of the optimization process. In order to make sure that the control remains bounded at T_0, it is required that

$$g_2|_{t=T_0} = g_{20}(x) \quad \text{on } \Gamma_a \qquad (8)$$

where $g_{20}(x)$ is a specified function defined on Γ_a. A logical choice is $g_{20}(x) = 0$ because the adjacent grid points yield this zero value.

2.2. The objective functional

Assume that Γ_s is a finite, connected part of the wall $[x \geq 0,\ y = 0]$ which is disjoint from Γ_a and that (T_a, T_b) is a time interval such that $0 \leq T_a < T_b \leq T$. Then, consider the functional

$$\mathcal{J}(u,v,p,g_2) = \frac{\alpha_2}{2}\int_{T_a}^{T_b}\int_{\Gamma_s}\left|-p + 2\nu\frac{\partial v}{\partial y} - \tau_2\right|^2 d\Gamma dt + \frac{\beta_2}{2}\int_{T_0}^{T_1}\int_{\Gamma_a}\left(\left|\frac{\partial g_2}{\partial t}\right|^2 + |g_2|^2\right) d\Gamma dt \qquad (9)$$

where g_2 denotes the control and $\tau_2(t,x)$ is a given function defined on $(T_a, T_b)\times\Gamma_s$. Note that since Γ_s is part of the lower boundary, $-p + 2\nu\partial v/\partial y$ is the normal stress, exerted by the fluid on the bounding wall along Γ_s and thus τ_2 may be interpreted as a given normal stress. Then, the boundary segment Γ_s can be thought of as a sensor which measures the stresses on the wall. Thus, in (9), Γ_s is the part of the boundary Γ along which one wishes to match the normal stress to the given function τ_2, and (T_a, T_b) is the time interval over which this matching is to take place.

The second term in (9) is used to limit the size of the control. Indeed, no bounds are *a priori* placed on g_2; its magnitude is limited by adding a penalty to the stress matching functional defined by the first term in (9). The particular form that these penalty terms take is motivated by the necessity to limit not only the size of the control g_2, but also to limit oscillations in time. The constants α_2 and β_2 are used to adjust the relative importance of the terms appearing in the functional (9).

The (constrained) optimization problem is given as follows:

Find $u, v, p,$ and g_2 such that the functional $\mathcal{J}(u,v,p,g_2)$ given in (9) is minimized subject to the requirement that (1)-(7) are satisfied.

3. THE OPTIMALITY SYSTEM

3.1. The Lagrangian functional

The method of Lagrange multipliers is formally used to enforce the constraints (1)-(3) and (5). To this end, the Lagrangian functional is introduced.

$$
\begin{aligned}
&\mathcal{L}(u,v,p,g_2,\hat{u},\hat{v},\hat{p},s_2)\\
&=\frac{\alpha_2}{2}\int_{T_a}^{T_b}\int_{\Gamma_s}\left|-p+2\nu\frac{\partial v}{\partial y}-\tau_2\right|^2 d\Gamma dt\\
&+\frac{\beta_2}{2}\int_{T_0}^{T_1}\int_{\Gamma_a}\left(\left|\frac{\partial g_2}{\partial t}\right|^2+|g_2|^2\right)d\Gamma dt\\
&-\int_0^T\int_\Omega \hat{u}\left(\frac{\partial u}{\partial t}+u\frac{\partial u}{\partial x}+v\frac{\partial u}{\partial y}+\frac{\partial p}{\partial x}-\nu\frac{\partial^2 u}{\partial x^2}-\nu\frac{\partial^2 u}{\partial y^2}\right)d\Omega dt\\
&-\int_0^T\int_\Omega \hat{v}\left(\frac{\partial v}{\partial t}+u\frac{\partial v}{\partial x}+v\frac{\partial v}{\partial y}+\frac{\partial p}{\partial y}-\nu\frac{\partial^2 v}{\partial x^2}-\nu\frac{\partial^2 v}{\partial y^2}\right)d\Omega dt\\
&-\int_0^T\int_\Omega \hat{p}\left(\frac{\partial u}{\partial x}+\frac{\partial v}{\partial y}\right)d\Omega dt-\int_{T_1}^T\int_{\Gamma_a} s_2 v\, d\Gamma dt\\
&-\int_{T_0}^{T_1}\int_{\Gamma_a} s_2(v-g_2)d\Gamma dt-\int_0^{T_0}\int_{\Gamma_a} s_2 v\, d\Gamma dt \qquad (10)
\end{aligned}
$$

In (10), $\hat{u}$ and $\hat{v}$ are Lagrange multipliers that are used to enforce the x and y-components of the momentum equation (1) and (2), respectively, $\hat{p}$ is a Lagrange multiplier that is used to enforce the continuity equation (3), and s_2 is a Lagrange multiplier that is used to enforce the y-component of the boundary condition (5). Note that Lagrange multipliers have not been introduced to enforce the constraints (4) and (6)-(8), so that these conditions must be required of all candidate functions u, v, p, and g_2.

Through the introduction of Lagrange multipliers, the constrained optimization problem is converted into the unconstrained problem:

> *Find u, v, p, g_2, $\hat{u}$, $\hat{v}$, $\hat{p}$, and s_2 satisfying (4) and (6)-(8) such that the Lagrangian functional $\mathcal{L}(u,v,p,g_2,\hat{u},\hat{v},\hat{p},s_2)$ given by (10) is rendered stationary.*

In this problem, each argument of the Lagrangian functional is considered to be an independent variable so that each may be varied independently.

The first-order necessary condition that stationary points must satisfy is that the first variation of the Lagrangian with respect to each of its arguments vanishes at those points. One easily sees that the vanishing of the first variations with respect to the Lagrange multipliers recovers the constraint equations (1)-(3) and (5). Specifically,

$$
\begin{aligned}
\frac{\delta\mathcal{L}}{\delta\hat{u}}=0 \quad &\Longrightarrow \quad x\text{-momentum equation (1)}\\
\frac{\delta\mathcal{L}}{\delta\hat{v}}=0 \quad &\Longrightarrow \quad y\text{-momentum equation (2)}\\
\frac{\delta\mathcal{L}}{\delta\hat{p}}=0 \quad &\Longrightarrow \quad \text{continuity equation (3)}\\
\frac{\delta\mathcal{L}}{\delta s_2}=0 \quad &\Longrightarrow \quad \text{wall-normal boundary condition (5)}
\end{aligned}
$$

where $\delta\mathcal{L}/\delta\hat{u}$ denotes the first variation of $\mathcal{L}$ with respect to $\hat{u}$, etc.

3.2. The adjoint equations

Next, set the first variations of the Lagrangian with respect to the state variables u, v, and p equal to zero. These result in the *adjoint* or *co-state equations*. Note that since candidate solutions must satisfy (4) and (6)-(8), one has that

$$
\begin{aligned}
&\delta u|_{t=0}=\delta v|_{t=0}=0 \quad \text{on } \Omega, \quad \delta g_2|_{t=T_0}=0 \quad \text{on } \Gamma_a,\\
&\delta u|_{\Gamma_i}=\delta v|_{\Gamma_i}=0; \quad \delta u|_{\Gamma_w}=\delta v|_{\Gamma_w}=0 \quad \text{for } (0,T),\\
&\delta p,\delta u,\delta v,\frac{\partial\delta u}{\partial x},\frac{\partial\delta v}{\partial x}\to 0 \text{ as } x\to\infty \text{ for } (0,T) \qquad (11)
\end{aligned}
$$

First, consider $\delta\mathcal{L}/\delta p=0$ which yields an equation for arbitrary variations δp in the pressure. Applying Gauss' theorem and choosing variations δp that vanish on the boundary Γ but which are arbitrary in the interior Ω of the flow domain yields

$$
\frac{\partial\hat{u}}{\partial x}+\frac{\partial\hat{v}}{\partial y}=0 \quad \text{on } (0,T)\times\Omega. \qquad (12)
$$

Next, consider $\delta\mathcal{L}/\delta u=0$ and $\delta\mathcal{L}/\delta v=0$. Apply Gauss' theorem enough times to remove all derivatives from the variation δu and δv in the integrals on Ω and use (11) to eliminate boundary integrals along Γ_i, Γ_w and as $x\to\infty$ and an integral over Ω at $t=0$. First, variations δv that vanish at $t=0$, $t=T$, and in a neighborhood of Γ are chosen, but which are otherwise arbitrary. Such a choice implies that all boundary integrals vanish giving

$$
\begin{aligned}
&-\frac{\partial\hat{u}}{\partial t}+\hat{u}\frac{\partial u}{\partial x}+\hat{v}\frac{\partial v}{\partial x}-u\frac{\partial\hat{u}}{\partial x}-v\frac{\partial\hat{u}}{\partial y}-\frac{\partial\hat{p}}{\partial x}\\
&\qquad -\nu\frac{\partial^2\hat{u}}{\partial x^2}-\nu\frac{\partial^2\hat{u}}{\partial y^2}=0 \quad \text{in } (0,T)\times\Omega \qquad (13)
\end{aligned}
$$

$$
\begin{aligned}
&-\frac{\partial\hat{v}}{\partial t}+\hat{u}\frac{\partial u}{\partial y}+\hat{v}\frac{\partial v}{\partial y}-u\frac{\partial\hat{v}}{\partial x}-v\frac{\partial\hat{v}}{\partial y}-\frac{\partial\hat{p}}{\partial y}\\
&\qquad -\nu\frac{\partial^2\hat{v}}{\partial x^2}-\nu\frac{\partial^2\hat{v}}{\partial y^2}=0 \quad \text{in } (0,T)\times\Omega \qquad (14)
\end{aligned}
$$

where equation (3) is used to effect a simplification. Next, variations that vanish in a neighborhood of Γ, but which are otherwise arbitrary, are chosen to obtain

$$(\hat{u},\ \hat{v})\big|_{t=T} = (0,0) \quad \text{in } \Omega\,. \tag{15}$$

Now, along Γ, δv and $\partial\delta v/\partial n$ may be independently selected, provided that (11) is satisfied, where $\partial/\partial n$ denotes the derivative in the direction of the outward normal to Ω along Γ. If $\delta v = 0$ and $\partial\delta v/\partial n$ varies arbitrarily along Γ, then

$$(\hat{u},\hat{v}) = (0,0) \ \text{ on } \begin{cases} (0,T)\times\Gamma_o, \Gamma_a, \Gamma_w\backslash\Gamma_s \\ (0,T_a)\times\Gamma_s \\ (T_b,T)\times\Gamma_s\,, \end{cases} \tag{16}$$

and

$$\begin{pmatrix}\hat{u}\\ \hat{v}\end{pmatrix} = -\begin{pmatrix} 0 \\ \alpha_2\left(-p+2\nu\frac{\partial v}{\partial y}-\tau_2\right)\end{pmatrix} \quad \text{on } (T_a,T_b)\times\Gamma_s\,, \tag{17}$$

where $\Gamma_w\backslash\Gamma_s$ denotes the boundary Γ_w with Γ_s excluded and Γ_o denotes the outflow boundary on the finite computational domain.

3.3. The optimality condition

The only first order necessary condition left to consider is $\delta\mathcal{L}/\delta g_2 = 0$. (These types of conditions are usually called the *optimality conditions.*) Now, since all candidate function g_2 must satisfy (8), it follows that $\delta g_2 = 0$ at $t = T_0$. Then with $\delta\mathcal{L}/\delta g_2 = 0$, applying Gauss' theorem to remove all derivatives from the variation δg_2 combined with $\delta g_2|_{t=T_0} = 0$, and choosing variations δg_2 that vanish at $t = T_1$ but which are otherwise arbitrary we find

$$-\frac{\partial^2 g_2}{\partial t^2} + g_2 = -\frac{1}{\beta_2}\left(\hat{p}+2\nu\frac{\partial\hat{v}}{\partial y}\right) \quad \text{on } (T_0,T_1)\times\Gamma_a \tag{18}$$

Now, choosing variations that are arbitrary at $t = T_1$ yields that $\partial g_2/\partial t = 0$ along Γ_a at $t = T_1$ so that, invoking (8), $g_2(t,x)$ satisfies

$$g_2|_{t=T_0} = g_{20}(x) \ \text{ and } \ \frac{\partial g_2}{\partial t}\Big|_{t=T_1} = 0 \quad \text{on } \Gamma_a \tag{19}$$

Note that, given $\hat{p}$ and $\hat{v}$, (18)-(19) constitute, at each point $x\in\Gamma_a$, a two-point boundary value problem in time over the interval (T_0,T_1).

3.4. Finite computational domain

In the computations, the semi-infinite domain Ω is replaced by a finite domain Ω_C. The convective unsteady flow problem described by the Navier-Stokes equations requires an outflow boundary Γ_o treatment that prevents numerical reflections. This buffer-domain technique described by Streett & Macaraeg (1989) is used here.

A similar treatment of inflow boundary Γ_i must be accounted for with the adjoint equations. In fact, the inflow boundary Γ_i for the state equation is the outflow boundary for the adjoint equations and, conversely, the outflow boundary Γ_o for the state equation is the inflow boundary for the adjoint equations because of the fact that t is increasing in the state equations and decreasing in the adjoint equations.

Due to (7), the allowable variations are further constrained to a relationship that implies that, along Γ_e, one may not choose the variations in δp and $\partial\delta v/\partial y$ independently. Considering, simultaneously, variations in p, v, and $\partial v/\partial y$ along Γ_e, it can be shown that one obtains

$$\hat{u} = 0 \quad \text{on } (0,T)\times\Gamma_e \tag{20}$$

Then, letting δv be arbitrary along Γ_e yields

$$\hat{p}+2\nu\frac{\partial\hat{v}}{\partial y}+v\hat{v} = 0 \quad \text{on } (0,T)\times\Gamma_e \tag{21}$$

The state equations (1)-(7) are driven by the given initial velocity (u_0,v_0), the given inflow velocity (u_i,v_i), and the controls $(0,g_2)$. Indeed, the purpose of this study is to determine g_2 that optimally counteracts instabilities created upstream of Γ_a. The adjoint equations (13)-(17) and (21) are homogeneous except for the boundary condition (17) along Γ_s, the part of the boundary along which we are trying to match the stresses. The data in that boundary condition is exactly the discrepancy between the desired stress τ_2 and the stress $-p+2\nu\partial u/\partial y$ along Γ_s, weighted by the factor α_2. The equations for the controls (18)-(19) are driven by the negative of the adjoint stress along Γ_a, the part of the boundary along which we apply the control, weighted by the factor $1/\beta_2$.

4. NUMERICAL EXPERIMENTS

Here, the optimal control methodology developed in Section 3 is applied to a boundary-layer flow having a single instability wave that can be characterized by a discrete frequency within the spectrum. We are not concerned with the details of how disturbances are ingested into the boundary layer; the underlying assumption here is that natural transition involves some dominant disturbances that can be characterized by waves, and in fact, in the present study, by a single wave. As described and reviewed by Joslin et al. (1994), these discrete small-amplitude instabilities can be suppressed through *wave cancellation* (WC), or wave superposition, using known exact information concerning the wave. Hence, the optimal control is "known" and can be

used to validate the present DNS/optimal control theory approach in which the instability is to be suppressed without any a priori knowledge of said instability.

The formidable coupled system (1)-(7) and (12)-(21) is solved in an iterative manner. First, the simulation starts with no control ($g_2 = 0$) and the Navier-Stokes equations are solved for the velocity (u, v) and pressure (p) fields. The adjoint equations are then solved for the co-state variables $(\hat{u}, \hat{v})$ and $\hat{p}$. Then, using these adjoint variables, the control g_2 is then found by solving the sub-system (18)-(19). The procedure is repeated until satisfactory convergence is achieved.

The nonlinear, unsteady Navier-Stokes equations and linear adjoint Navier-Stokes equations are solved by direct numerical simulation (DNS) of disturbances that evolve spatially within the boundary layer. The spatial DNS approach (Joslin et al. 1993) involves spectral and high-order finite-difference methods and a three-stage Runge-Kutta method for time advancement. Disturbances are forced into the boundary layer by unsteady suction and blowing through a slot in the wall upstream of the actuator.

4.1. Computational Parameters

For the computations, the grid has 401 streamwise and 41 wall-normal points. The free-stream boundary is located $75\delta_o^*$ from the wall, and the streamwise length is $224\delta_o^*$ which is equal to approximately 8 Tollmien-Schlichting (TS) wavelengths. The nondimensional frequency for the forced disturbance is $F = \omega/R \times 10^6 = 86$; the forcing amplitude is $v_f = 0.1\%$. The Reynolds number based on the inflow displacement thickness (δ_o^*) is $R = 900$. (The boundary segment along which disturbance forcing and control is effected as well as where stress matching occurs are located within the unstable region of the linear stability neutral curve.) A time-step size corresponding to 320 steps per period T_p is chosen for a three-stage Runge-Kutta method. Based on the disturbance frequency, a characteristic period can be defined as $T_p = 2\pi/\omega = 81.1781$; the resulting time-step size is then $\Delta t = 0.2537$.

To complete one period of the active-control simulation process, 45 seconds on a Cray C-90 are required using a single processor. Note, two periods of cost ($T_a \rightarrow T_b$ and $T_b \rightarrow T_a$) are required to complete one iteration of the DNS/adjoint system. Although in general any time interval may be specified for $T_a \rightarrow T_b$, this study uses integer increments of the period (T_p) for simplicity. Hence, $T_a \rightarrow T_b = 2T_p$ would cost $4T_p$ in computations, or roughly 3 min of C-90 time per iteration. Because only a single small-amplitude wave (linear) is forced, the above grid is more than adequate; however, a grid refinement was performed and produced results equivalent to the results reported here.

For this study, the disturbance forcing slot Γ_f, the control or actuator orifice Γ_a, and the matching or sensor segment Γ_s have equal length $4.48\delta_o^*$. The forcing is centered downstream at $389.62\delta_o^*$ (the Reynolds number based on the displacement thickness at that location is $R = 1018.99$), the actuator is centered at $403.62\delta_o^*$ ($R = 1037.13$), and the sensor is centered at $417.62\delta_o^*$ ($R = 1054.97$). These separation distances were arbitrarily chosen for this demonstration. In practice, the control and matching segments should have a minimal separation distance so that the pair can be packaged as a single unit, or bundle, for distributed application of many bundles.

4.2. Results

All simulations allow the flow field to develop for one period; i.e., from $t = 0 \rightarrow T_a = T_p$, before control is initiated. In the first series of simulations, the interval during which control is applied is arbitrarily chosen to be $T_a \rightarrow T_b = 2T_p$. Based on $\alpha_2 = 1$ and $\beta_2 = 10$, the convergence history for the wall-normal velocity (v) and the actuator response g_2 is shown in Fig. 1. The velocities are obtained at a fixed distance from the wall corresponding to $1.18\delta_o^*$ and are obtained at the fixed time T_b. Convergence is obtained with 4 iterations. The results demonstrate that a measure of wave cancellation can be obtained from the DNS/control theory system. The wall-normal amplitude of the modified wave at $R = 1092.5$ is 40 percent of the uncontrolled wave; the control without optimizing the choice of α_2 and β_2 has led to a 60 percent decrease in the amplitude of the travelling wave. This results in a delay of transition by-way-of a suppression of the instability evolution. The converged results for this case are referred to as C1.

The effect of varying the window size (T_a, T_b) was examined by comparing the converged results (C1) which has a window length ($T_a = T_p \rightarrow T_b = 2T_p$) with converged results (C2) for the extended window ($T_a = T_p \rightarrow T_b = 3T_p$). The results are identical for the first two periods of time and indicate that extending the amount of time for control serves to extend control only. This result also indicates that one can solve for the optimal control over a given time interval (T_a, T_b) by breaking up that interval and solving for the optimal control over a series of smaller subintervals. This approach could lead to substantial savings in CPU and memory costs.

The instability wave resulting from wave cancellation (WC) is shown with the control (C2) in Fig. 2. For the present comparison, the amplitude of the actuation for WC was adjusted until nearly exact wave cancellation was achieved. Although the DNS/control theory did not achieve the same level of energy removal, the similar effect of WC was achieved without any a priori knowledge of the instability. Also, note that g_2 shows that the optimal state of the control theory has nearly the exact phase characteristics as WC and only lacks the necessary amplitude for additional

wave cancellation. These encouraging results suggest that by the appropriate selection of α_2 and β_2, the optimal control would be as effective for instability suppression as exact wave cancellation.

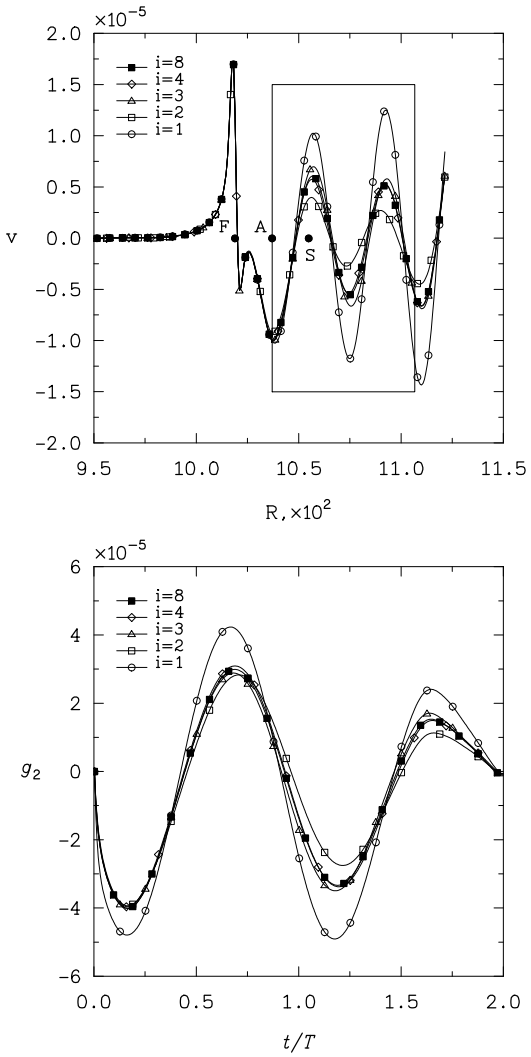

Figure 1. Convergence of disturbance wall-normal velocity and actuator response with downstream distance for control (C1) in flat-plate boundary-layer flow.

From the wave-cancellation study of Joslin et al. (1994), the relationship between amplitude of the actuator (v_a) and resulting instability showed a similar result found in the channel flow wave-cancellation study of Biringen (1984). Figure 3 shows this relationship. Beginning with a small actuation amplitude, as the actuation level is increased, the amount of wave cancellation (energy extraction from the disturbance) increases. At some optimal actuation, nearly exact wave cancellation is achieved for the instability wave. As the actuation amplitude further increases the resulting instability amplitude increases; this was clearly explained in Joslin et al. (1994) to occur because in the wave superposition process, the actuator wave becomes dominant over the forced wave. At this point, the resulting instability undergoes a phase shift corresponding to the phase of the wave generated by the actuator. The relationship is encouraging for the DNS/optimal control theory approach and suggests that a gradient descent type algorithm might further enhance the wave suppression capability of the present approach. Namely, an approach for the optimal selection of α_2 and β_2 might lead to a more useful theoretical/computational tool for flow control. In practice, this optimal selection would be accomplished through a feedback loop.

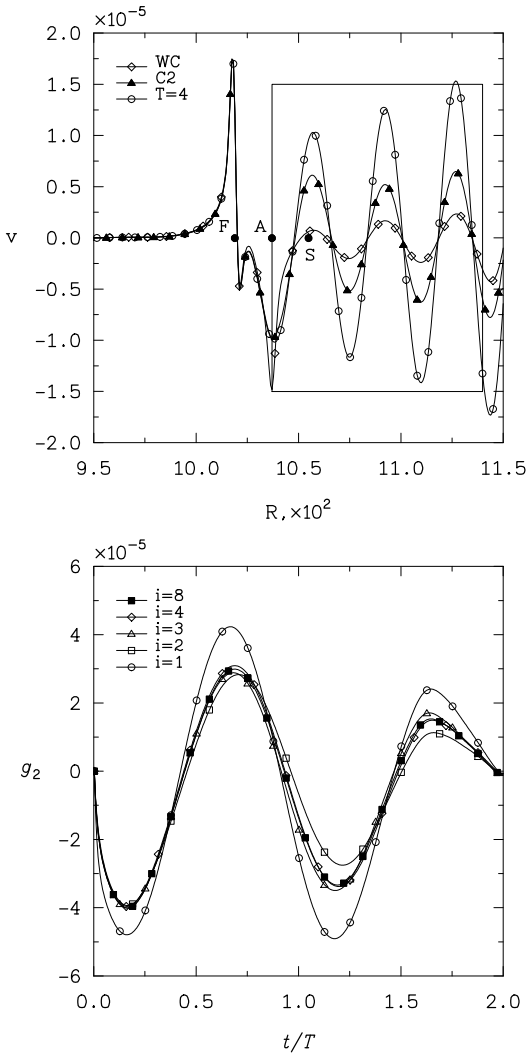

Figure 2. Disturbance wall-normal velocity and actuator response with downstream distance for control (C2) and wave cancellation (WC).

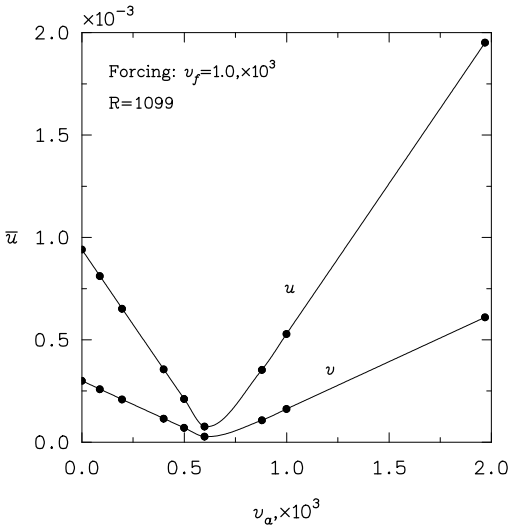

Figure 3. Disturbance velocity resulting from variations in actuator amplitude from simulations in Joslin et al. (1994).

To simply demonstrate this concept, Lagrange interpolation (or perhaps extrapolation) is introduced for β_2 based on imposed value for α_2:

$$\beta_2^{n+1} = \frac{\beta_2^n(\tau_2^* - \tau_2^{n-1}) - \beta_2^{n-1}(\tau_2^* - \tau_2^n)}{(\tau_2^n - \tau_2^{n-1})}, \qquad (22)$$

where τ_2^* are some desired values of the stress components and τ_2^n are the stress components based on the choice β_2^n. Although τ_2^* may be equivalent to the target value τ_2 in the functional (11), this may lead to significant over/under shoots during the iteration process. Instead, τ_2^* is the incremental decrease, or target value, for interpolation to more desirable and β_2 values. To illustrate this process, the $\beta_2 = 10$ (C2) and $\beta_2 = 11$ control results are obtained with the iteration procedure. The measures of normal stress are somewhat arbitrarily obtained at some time as measured by the sensor or matching segment Γ_s; the values of the normal stress are given in the Table 1. These values are used for a desired normal stress τ_2^*, which in this case is 65% of the $\beta_2 = 11$ results.

Table 1. Normal stress for two values of β_2.

β_2	normal stress
10	9.369×10^{-6}
11	8.814×10^{-6}

Using the results for $\beta_2 = 10$ and $\beta_2 = 11$ in (22) yields the value $\beta_2 = 16.5$ which is used in a simulation to obtain a greater degree of instability suppression. The WC results and the enhanced optimal control (C3) solution are shown in Fig. 4. This interpolation approach indicates that optimizing β_2 has led to results comparable to WC. For all practical purposes, the solutions obtained with the present DNS/control theory methodology yield the desired flow control features without prior knowledge of the forced instability.

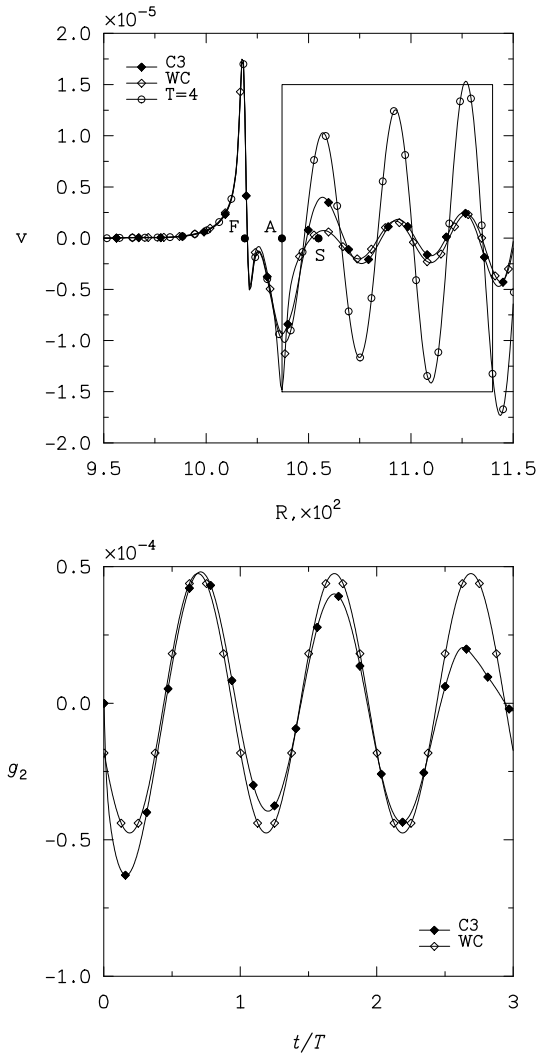

Figure 4. Disturbance wall-normal velocity and actuator response with downstream distance for control (C3) and wave cancellation (WC).

The adjoint system requires that the velocity field (u, v) obtained from the Navier-Stokes equations be known for all time. For the iteration sequence and a modestly course grid, 82 Mbytes of disk (or runtime) space are required to store the velocities at all time steps and for all grid points for one period. For $T_a \rightarrow T_b = 3T_p$, 246 Mbytes are necessary for the computation. Clearly for three-dimensional problems the control scheme becomes prohibitively expensive. Therefore, a secondary goal of this study is to determine if this limitation can be eliminated. Because the characteristics of the actuator (g_2) and resulting solutions are compara-

ble to WC, some focus should be placed on eliminating this large memory requirement. This limitation can easily be removed if the flow-control problem involves small-amplitude unsteadiness (or instabilities). The time-dependent coefficients of the adjoint system reduce to the steady-state solution and no addition memory is required over the Navier-Stokes system in terms of coefficients. This has been verified by a comparison of a simulation with steady coefficients compared with the C2 control case (see Joslin et al., 1995). Additionally, if the instabilities have small amplitudes, then a linear Navier-Stokes solver can be used instead of the full nonlinear solver, which was used in the present study. This linear system would be very useful for the design of flow-control systems. However, if the instabilities in the flow have sufficient amplitude to interact nonlinearly, then some measure of unsteady coefficient behavier is likely required. Depending on the amplitudes, the coefficients saved at every time-step may be replaced with storing coefficients every 10 or more time-steps or with some statistical average of the flow, thereby reducing the memory requirements by an order of magnitude. This hypothesis will require validation in a future study.

CONCLUSIONS

The coupled Navier-Stokes equations, adjoint Navier-Stokes, and optimality condition equations were solved and validated for the flow-control problem of instability wave suppression in a flat plate boundary-layer flow. By solving the above system, optimal controls were determined that met the objective of minimizing the perturbation normal stress along a portion of the bounding wall. As a result, the optimal control was found to be an effective means for suppressing two-dimensional, unstable Tollmien-Schlichting travelling waves. The results indicate that the DNS/control theory solution is comparable to the wave-cancellation result but, unlike the latter, requires no a priori knowledge of the instability characteristics.

ACKNOWLEDGEMENTS

This research was supported by NASA under contract no. NAS1-19480 while the authors (except the first author) were in residence at the Institute for Computer Applications in Science and Engineering, NASA Langley Research Center, Hampton, VA. Max Gunzburger was also supported by the Air Force Office of Scientific Research under grant number AFOSR-93-1-0280.

REFERENCES

Biringen, S., 1984, "Active Control of Transition by Periodic Suction-Blowing," *Physics of Fluids*, Vol. 27, No. 6, pp. 1345-1347.

Gad-el-Hak, M., 1989, "Flow Control," *Applied Mechanics Reviews*, Vol. 42, No. 10, pp. 261-293.

Gad-el-Hak, M. and Bushnell, D. M., 1991, "Separation Control: Review," *Journal of Fluids Engineering*, Vol. 113, pp. 5-30.

Joslin, R. D., Streett, C. L. & Chang, C.-L., 1993, "Spatial Direct Numerical Simulation of Boundary-Layer Transition Mechanisms: Validation of PSE Theory," *Theoretical & Computational Fluid Dynamics*, Vol. 4, pp. 271-288.

Joslin, R. D., Erlebacher, G. & Hussaini, M. Y., 1994, "Active Control of Instabilities in Laminar Boundary-Layer Flow. An overview," NASA CR 195016, ICASE Report No. 94-97, December 1994.

Joslin, R. D., Gunzburger, M. D., Nicolaides, R.A., Erlebacher, G. & Hussaini, M. Y., 1995, "A Self-Contained, Automated Methodology for Optimal Flow Control Validated for Transition Delay," NASA CR 198215, ICASE Report No. 95-64, September 1995.

Streett, C. L. & Macaraeg, M. G., 1989, "Spectral Multi-Domain for Large-Scale Fluid Dynamics Simulations," *Applied Numerical Mathematics*, Vol. 6, pp. 123-140.